ACS Medicinal Chemistry Letters

pubs.acs.org/acsmedchemlett

Discovery of MK-5046, a Potent, Selective Bombesin Receptor Subtype-3 Agonist for the Treatment of Obesity

Iyassu K. Sebhat,*[,†] Christopher Franklin,[†] Michael M.-C. Lo,[†] David Chen,[†] James P. Jewell,[†] Randy Miller,[‡] Jianmei Pang,[‡] Oksana Palyha,[§] Yanqing Kan,[§] Theresa M. Kelly,[§] Xiao-Ming Guan,[§] Donald J. Marsh,[§] Jennifer A. Kosinski,[§] Joseph M. Metzger,[∥] Kathryn Lyons,[‡] Jasminka Dragovic,[‡] Peter R. Guzzo,[⊥] Alan J. Henderson,[⊥] Marc L. Reitman,[§] Ravi P. Nargund,[†] Matthew J. Wyvratt,[†] and Linus S. Lin[†]

Departments of [†]Medicinal Chemistry, [‡]Drug Metabolism, [§]Metabolic Diseases (Obesity), and [∥]Pharmacology, Merck Research Laboratories, Rahway, New Jersey 07065, United States, and [⊥]AMRI, 26 Corporate Circle, Albany, New York 12212, United States

ABSTRACT We report the development and characterization of compound **22** (MK-5046), a potent, selective small molecule agonist of BRS-3 (bombesin receptor subtype-3). In pharmacological testing using diet-induced obese mice, compound **22** caused mechanism-based, dose-dependent reductions in food intake and body weight.

KEYWORDS MK-5046, bombesin receptor subtype-3 agonist, obesity

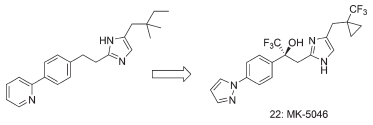

The mammalian bombesin G-protein-coupled receptor subfamily[1] comprises three structurally related members, the receptors for neuromedin B (NMBR or BB1), gastrin-releasing peptide (GRPR or BB2),[2] and bombesin receptor subtype-3 (BRS-3 or BB3).[3] BRS-3 is an orphan receptor whose natural ligand is not known and which, despite its name, does not bind bombesin with high affinity. BRS-3 is expressed predominantly in the central nervous system (CNS). Mice lacking functional BRS-3 develop mild obesity and insulin resistance, suggesting a role for the receptor in the regulation of energy homeostasis.[4] In addition, BRS-3 as well as the other mammalian family members are expressed by several human carcinoma cell lines, where they may play a role in growth regulation.[3] Until recently, there have been limited reports of peptide[5] or small-molecule[6−9] pharmacological tools to further elucidate the role of the receptor and determine its potential as a drug target.

Our laboratory has described the lead identification and initial optimization of the first reported series of small-molecule BRS-3 agonists with efficacy in body weight lowering.[10−12] Exploratory medicinal chemistry efforts focused on lead **1**. The potency at the human receptor was improved through the incorporation of branched substituents at the 4-position of the imidazole, while systemic and CNS exposure were increased through replacement of the benzoic acid moiety with pyridine. This work eventually led to the identification of **2** (Bag-1), the first key pharmacological tool in our program. Results of in vivo testing with this compound furnished a preclinical proof of concept for the BRS-3 mechanism: Administration of the BRS-3 agonist in established diet-induced obese (eDIO) mice caused a significant reduction of acute food intake and increase in fasting metabolic rate, and these effects were not evident in *Brs3* null (KO) mice.[13] Furthermore, subchronic dosing (100 mpk BID, 8 days) led to mechanism-based body weight lowering in eDIO mice, while it had no significant effects in KO mice.[13]

Undesirable features of **2** were its poor oral pharmacokinetics in preclinical species and a suboptimal off-target profile that included low micromolar binding to the human inward rectifying potassium ion channel (hERG, IC_{50} = 1.2 μM) as well as the diltiazem (DLZ) site of the rabbit calcium ion channel (IC_{50} = 0.5 μM).

The low unbound exposure of compound **2** was shown to be due primarily to high intrinsic clearance. A bile duct cannulated rat study was performed to examine the fate of the compound after in vivo dosing. For this purpose, a tritium radiolabel was incorporated in the 5-position of the pyridine ring. Biliary excretion of metabolized **2** accounted for ~65% of the recovered radioactivity after both iv and po dosing, suggesting good absorption. There was extensive hydroxylation and concomitant loss of the radiolabel, suggesting oxidative metabolism of the pyridine ring. In addition, hydroxylation of both the 2-substituent (ethyl linker) and the 4-substituent (branched alkyl chain) of the imidazole was observed. Together, these oxidative processes were the cause for the poor pharmacokinetic profile of these early leads.

To advance the series, we searched for motifs that might furnish more metabolically stable structures for further structure−activity relationship (SAR) and identified analogue **3** bearing a 5-fluoropyridine. When we assessed the stability of this compound by incubation with rat liver

Received Date: August 19, 2010
Accepted Date: October 6, 2010
Published on Web Date: October 18, 2010

DOI: 10.1021/ml100196d | *ACS Med. Chem. Lett.* **2011**, *2*, 43–47

ACS Medicinal Chemistry Letters
pubs.acs.org/acsmedchemlett

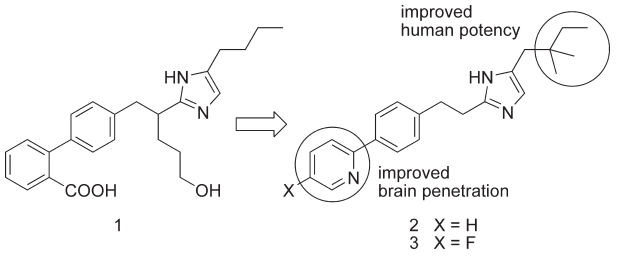

Figure 1. Structures of leads **1**−**3**.

Table 1. Human BRS-3 Activity and Rat Liver Microsomal (RLM) Stability of **1**−**3**

compd	hBRS-3[a] EC_{50} (nM) (% act)[b]	$T_{1/2}$ (RLM incubation) (min)
1	1900 ± 760 (74 ± 33%)	ND[c]
2	47 ± 4 (99 ± 4%)	1
3	66 ± 16 (97 ± 4%)	3

[a] Data expressed as means ± SDs (≥3 independent experiments). [b] % act represents the maximum activation of tested compound relative to that of the dY peptide {[D-Tyr^6,β-Ala^{11},Phe^{13},Nle^{14}]bombesin(6−14)}. [c] Not determined.

microsomes, it had an improved half-life in comparison with **2**. However, off-target activities remained problematic, with reduced selectivity vs the two key ion channels (hERG, K_i = 0.4 μM; DLZ, IC_{50} = 0.2 μM), as well as some activation of human PXR (IC_{50} = 3.5 μM with 44% maximal activation).

More information was garnered from early SAR focused on the imidazole substituent: In a survey of branched alkyl groups, use of a 2,2-dimethylpropane in place of the 2,2-dimethylbutane contained in compounds **2** and **3** resulted in ∼4-fold reduction in activity at human BRS-3. While a loss in potency and selectivity is not ideal, we considered it a small price to pay for increased metabolic stability and proceeded to incorporate the fluoropyridine and truncated substituent.

We next aimed to improve the selectivity for BRS-3 over off-target effects by introducing heteroatom substituents on the central ethylene linker to increase polarity and reduce the number of low energy, unfavorable configurations for the central ethyl linker region. We envisaged that such substitutions would also improve metabolic stability, given that the benzylic C−H would no longer be available for oxidation. Other attempts to further reduce metabolism in the pyridine region focused on incorporation of alternate heterocycles. Finally, we sought to further address the metabolism of the branched alkyl chain by incorporating metabolically more stable fluoroalkyl and cyclopropyl modifications.

Modular syntheses were developed to access the desired compounds. Both approaches relied on the deprotonation of suitably substituted imidazole precursors and their subsequent reaction with electrophiles.

To access the series of compounds with substituents attached to the carbon adjacent to the imidazole, 2-lithiated imidazoles were reacted with esters to generate ketone intermediates. For the purposes of the current series, reaction of 3,3-dimethylbutyraldehyde (**4**) with TosMIC generated 4-(2,2-dimethylpropyl)-1*H*-imidazole, which was subsequently protected as the

Scheme 1[a]

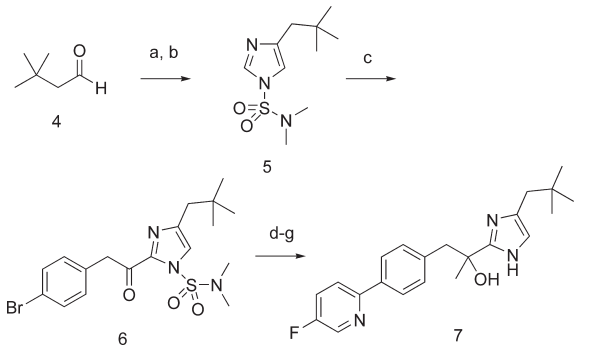

[a] Reagents and conditions: (a) (i) TosMIC, KO*t*Bu, THF; (ii) NH_3, MeOH. (b) Me_2NSO_2Cl, NMM, DME. (c) (i) *n*-BuLi, THF; (ii) 4-bromophenylacetic acid methyl ester, THF. (d) $Pd(PPh_3)_4$, 2-bromo-5-fluoropyridine, $Me_3SnSnMe_3$, dioxane. (e) MeMgBr, THF. (f) HCl, MeOH. (g) Chiral separation (Chiralpak AD-H, IPA/heptane).

Scheme 2[a]

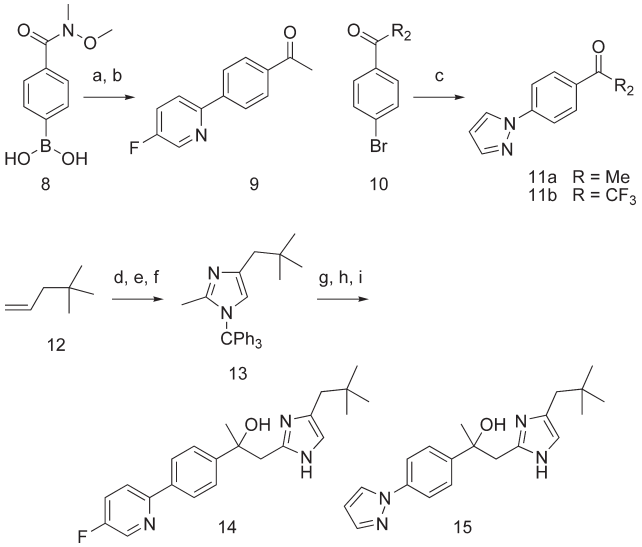

[a] Reagents and conditions: (a) $Pd(PPh_3)_4$, 2-bromo-5-fluoropyridine, K_2CO_3, toluene/MeOH. (b) MeMgBr, THF. (c) Compound **11a**: 4-bromoacetophenone, K_2CO_3, *rac-trans-N,N′*-dimethylcyclohexane-1,2-diamine (cat.), CuI (cat.), pyrazole, toluene; **11b**: 4′-bromo-2,2,2-trifluoromethylacetophenone, K_2CO_3, *rac-trans-N,N′*-dimethylcyclohexane-1,2-diamine (cat.), CuI (cat.), pyrazole, toluene (d) $NO^+BF_4^-$, MeCN. (e) $TiCl_3$, MeOH (f) Ph_3CCl, Et_3N, CH_2Cl_2. (g) (i) *n*-BuLi, THF; (ii) **9** or **11**, THF. (h) HCl, dioxane. (i) Chiral separation (Chiralpak AD-H, IPA/heptane).

dimethylsulfamoyl derivative **5**. Lithiation of **5**, followed by its reaction with methyl 4-bromophenylacetate, led to ketone **6**, which was coupled to the stannane generated in situ from 2-bromo-5-fluoropyridine via palladium catalysis. Finally, the addition of methylmagnesium bromide, deprotection, and chiral separation afforded two enantiomeric alcohols. Compound **7** is the more potent isomer.

To access the series with substituents attached to the carbon distal from the imidazole, 1-trityl-2-methyl-4-(2,2-dimethylpropyl)imidazole, synthesized in three steps from

DOI: 10.1021/ml100196d | *ACS Med. Chem. Lett.* **2011**, *2*, 43–47

Scheme 3[a]

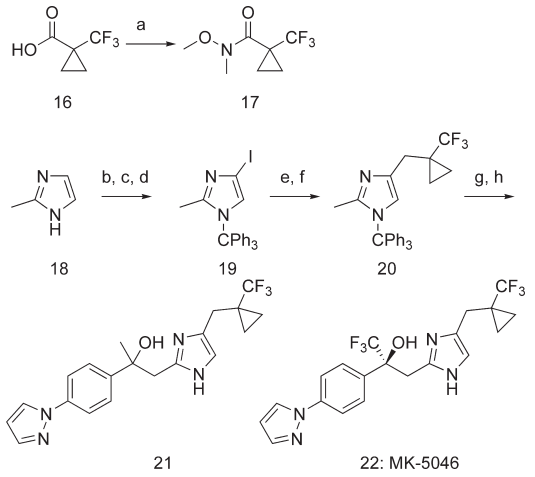

[a] Reagents and conditions: (a) MeONHMe, EDC, HOBt, NMM, CH_2Cl_2. (b) Na_2CO_3, I_2, dioxane/H_2O. (c) Na_2SO_3, EtOH/H_2O. (d) Ph_3CCl, Et_3N, CH_2Cl_2. (e) (i) EtMgBr, CH_2Cl_2; (ii) **17**, CH_2Cl_2. (f) H_2NNH_2, KOH, ethylene glycol. (g) (i) BuLi, THF; (ii) **11a** or **11b**, THF. (h) HCl, dioxane. (i) Chiral separation (Chiralpak AD-H, IPA/heptane).

Table 2. Human BRS-3 Binding and Functional Potency for Compounds **3**–**22**

compd	hBRS-3[a] IC_{50} (nM)	hBRS-3[a] EC_{50} (nM) (% act)[b]
3	16 ± 6	66 ± 16 (97 ± 4%)
7	82 ± 16	220 ± 22 (99 ± 4%)
14	17 ± 5	67 ± 13 (99 ± 2%)
15	5 ± 1	16 ± 3 (94 ± 5%)
21	11 ± 2	14 ± 4 (94 ± 6%)
22	27 ± 13	25 ± 3 (102 ± 6%)

[a] Data expressed as means ± SDs (≥3 independent experiments). [b] % act represents the maximum activation of tested compounds relative to that of dY peptide.

4,4-dimethylpentene, was lithiated in the α-position via treatment with *n*-butyllithium and subsequently reacted with methylaryl ketones **9** and **11a** or the trifluorinated analogue **11b**. As before, deprotection and chiral separation furnished agonists **14** and **15**. Similarly, the use of the trityl-protected imidazole **20** (derived in five steps from 2-methylimidazole) led to compounds **21** and **22**.[14]

Human BRS-3 binding potency and functional potency for the compounds are summarized in Table 2.[15] The introduction of a tertiary alcohol on either carbon of the linker resulted in compounds that maintained similar activity to lead **3**. Substitution distal from the imidazole (**14** vs **7**) gave slightly higher potency. Compounds **7** and **14** afforded improved off-target profiles relative to **3**. In particular, binding to the hERG potassium channel was diminished (K_i = 5.9 and 4.2 μM for **7** and **14**, respectively).

The initial leads **7** and **14** were assessed in rat pharmacokinetic studies. Although compound **7** had lower in vivo rat plasma clearance than **14** (14 vs 28 mL/min/kg), the unbound fraction (F_u) in plasma was considerably lower,

Table 3. Rat Plasma Clearance,[a] Protein Binding,[b] and Stability[c] for Compounds **3**–**22**

	rat in vivo		rat microsomal incubation	
compd	Cl_p (mL/min/kg)	plasma F_u (%)	$T_{1/2}$ (min)	F_u (%)
3	12	ND	3	ND[d]
7	14	0.1	1	20
14	28	0.4	5	20
15	110	6.8	ND	ND
21	52	3.2	ND	ND
22	20	1.0	ND	ND

[a] Plasma clearance (Cl_p) calculated following 1 mg/kg iv dose. [b] Protein binding assessed using human plasma (200 μL) or microsomal proteins (0.2 mg/mL) and test compound (1 μM). [c] Microsomal stability assessed using liver microsomes (0.2 mg protein/mL) and test compound (1 μM). [d] Not determined.

Table 4. Dog Pharmacokinetic Data[a] for Pyrazole Analogues **21** and **22**

compd	Cl_p (mL/min/kg)	$T_{1/2}$ (h)	po AUC_N [μM h/(mg/kg)]	F_{oral} (%)
21	10	0.3	1.4	29
22	5.6	1.4	3.7	52

[a] Plasma clearance (Cl_p) and half-life ($T_{1/2}$) calculated following 0.5 mg/kg iv dose. Normalized oral exposure (po AUC_N) and oral bioavailability (F_{oral}) calculated following 1 mg/kg po dose.

suggesting higher intrinsic clearance. This was reinforced in studies assessing the stability of the compounds in incubations with rat liver microsomes. The half-life for compound **7** was significantly shorter than that for compound **14**, indicating its propensity for higher metabolic intrinsic clearance (the two had similar unbound fractions under the conditions of the assay; F_u = 20%). On this basis, we focused our efforts on analogues of **14**, leading to the identification of pyrazole **15** with improved human potency. The rat pharmacokinetic profile of **15** was notable for very high total clearance, which was largely a function of increased plasma unbound fraction as compared to the other compounds. To further reduce the potential for oxidative metabolism, our attention turned to the remaining region (common to compound **2**) that was identified to be susceptible to oxidation in rats: the imidazole 4-substituent. After considerable efforts, trifluoromethyl-substituted methyl cyclopropane was incorporated to furnish compound **21**, where both the unbound fraction in rat plasma and the plasma clearance were reduced.

The pharmacokinetic properties of **21** were also evaluated in the dog where the half-life was found to be unacceptably short (Table 4). Replacement of the remaining methyl group with a trifluoromethyl group gave **22**. The compound exhibits overall improvements in dog pharmacokinetic properties relative to **21**, while maintaining good potency and improved selectivity over off-target activities (hERG potassium channel binding K_i > 8 μM).

Compound **22** was evaluated in a screen of >100 receptors, ion channels, and enzymes. Eight off-target activities were identified with IC_{50} values in the range of 0.5–10 μM,

DOI: 10.1021/ml100196d | *ACS Med. Chem. Lett.* 2011, *2*, 43–47

Table 5. BRS-3 Potency, Selectivity,[a] and Pharmacokinetic[b] Profile of **22** (MK-5046)

	human	mouse	rat	dog	rhesus
BRS3 IC_{50} (nM)	28 ± 13	5.4 ± 2	1.2 ± 0.4	6.5 ± 1.9	50 ± 15
BRS3 K_i (nM)	3.7 ± 0.5	1.6 ± 0.7	0.6 ± 0.2	9.9 ± 1.3	2.4 ± 1.3
BRS3 EC_{50} (nM)	14 ± 4	21 ± 0.9	2.2 ± 1	1.6 ± 0.8	6.9 ± 4
% activation[c]	100 ± 6	120 ± 10	110 ± 9	100 ± 58	110 ± 8
NMBR IC_{50} (nM)	> 10000				
GRPR IC_{50} (nM)	> 10000				
hERG K_i (μM)	> 8				
DLZ IC_{50} (μM)	1.9				
hPXR EC_{50} (μM)	> 25				
po AUC_N [μM h/(mg/kg)]		0.1	1.2	3.7	0.8
F_{oral} (%)		9.6	64	52	18
Cl_p (mL/min/kg)		32	20	5.6	8.8
Vd_{ss} (L/kg)		2.2	0.98	0.45	0.44
$T_{1/2}$ (h)		1.1	0.7	1.4	1.0

[a] Data expressed as means ± SDs (≥3 independent experiments) or single value. [b] Plasma clearance (Cl_p), volume of distribution (Vd_{ss}), and half-life ($T_{1/2}$) calculated following 1 mg/kg iv dose in mouse and rat and 0.5 mg/kg iv dose in dog and rhesus. Oral bioavailability (F_{oral}) calculated following 2 mg/kg in mouse and rat and 1 mg/kg in dog and rhesus. [c] % activation represents the maximum activation of tested compounds relative to that of dY-peptide for human, dog, and rhesus receptors and a reference small molecule BRS-3 agonist for mouse and rat receptors.

but none were considered significant enough to preclude the use of the compound as a pharmacological tool or for clinical development.

The BRS-3 potency and pharmacokinetic parameters for **22** across a range of species, as well as activity of the compound in selected off-target assays are summarized in Table 5. Potency, selectivity, and pharmacokinetics were all significantly improved as compared to compound **3**, and while the half-life remained relatively short, this was partially ameliorated by prolonged absorption, thereby allowing oral dosing paradigms in pharmacological studies.

Compound **22** was assessed for acute efficacy in wild-type (WT) and *Brs3* KO mice. In WT mice, the compound caused significant reductions in food intake and increase in fasting metabolic rate with no effect in the KO mice. After subchronic dosing in eDIO mice, compound **22** (25 mg/kg/day by sc infusion) caused reductions in body weight (8−9% as compared to vehicle-dosed animals) that were sustained for 14 days with no evidence of tachyphylaxis (manuscript submitted[16]).

In summary, a SAR about the core of lead compound **2** has resulted in the identification of a series of BRS-3 agonists with improved potency, selectivity, and oral exposure in preclinical species. On the basis of the in vitro and pharmacokinetic profiles, compound **22** (MK-5046) was chosen for further pharmacological study. In eDIO mice, sustained body weight loss was observed following 14 days of treatment with the compound. The data suggest that agonism of the BRS-3 may present a useful treatment for obesity, and compound **22** presents a suitable candidate for clinical investigation.

SUPPORTING INFORMATION AVAILABLE

Full experimental procedures and characterization data. This material is available free of charge via the Internet at http://pubs.acs.org.

AUTHOR INFORMATION

Corresponding Author: *Tel: 732-594-0168. E-mail: iyassu_sebhat@merck.com.

ACKNOWLEDGMENT

We thank the department of Laboratory Animal Resources for their assistance in animal dosing and sampling.

REFERENCES

(1) Jensen, R. T.; Battey, J. F.; Spindel, E. R.; Benya, R. V. Mammalian bombesin receptors: Nomenclature, distribution, pharmacology, signaling, and functions in normal and disease states. *Pharmacol. Rev.* **2008,** *60*, 1–42.

(2) Battey, J.; Wada, E. Two distinct receptor subtypes for mammalian bombesin-like peptides. *Trends Neurosci.* **1991,** *14*, 524–528.

(3) Fathi, Z.; Corjay, M. H.; Shapira, H.; Wada, E.; Benya, R.; Jensen, R.; Viallet, J.; Sausville, E. A.; Battey, J. F. BRS3: A novel bombesin receptor subtype selectively expressed in testis and lung carcinoma cells. *J. Biol. Chem.* **1993,** *268*, 5979–5984.

(4) Ohki-Hamazaki, H.; Watase, K.; Yamamoto, K.; Ogura, H.; Yamano, M.; Yamada, K.; Maeno, H.; Imaki, J.; Kikuyama, S.; Wada, E.; Wada, K. Mice lacking bombesin receptor subtype-3 develop metabolic defects and obesity. *Nature* **1997,** *390*, 165–169.

(5) Boyle, R. G.; Humphries, J.; Mitchell, T.; Showell, G. A.; Apaya, R.; Iijima, H.; Shimada, H.; Arai, T.; Ueno, H.; Usui, Y.; Sakaki, T.; Wada, E.; Wada, K. The design of a new potent and selective ligand for the orphan bombesin receptor subtype 3 (BRS3). *J. Pept. Sci.* **2005,** *11*, 136–141 and references therein.

(6) Weber, D.; Berger, C.; Heinrich, T.; Eickelmann, P.; Antel, J.; Kessler, H. Systematic optimization of a lead-structure identities for a selective short peptide agonist for the human orphan receptor BRS-3. *J. Pept. Sci.* **2002,** *8*, 461–475.

(7) Weber, D.; Berger, C.; Eickelmann, P.; Antel, J.; Kessler, H. Design of Selective Peptidomimetic Agonists for the Human Orphan Receptor BRS-3. *J. Med. Chem.* **2003,** *46*, 1918–1930.

(8) Carlton, D. L.; Collin-Smith, L. J.; Daniels, A. J.; Deaton, D. N.; Goetz, A. S.; Laudeman, C. P.; Littleton, T. R.; Musso, D. L.; Ott Morgan, R. J.; Szewczyk, J. R.; Zhang, C. Discovery of small molecule agonists for the bombesin receptor subtype 3 (BRS-3)

DOI: 10.1021/ml100196d | *ACS Med. Chem. Lett.* 2011, *2*, 43–47

based on an omeprazole lead. *Bioorg. Med. Chem. Lett.* **2008,** *18*, 5451–5455.
(9) Guo, C.; Guzzo, P. R.; Hadden, M.; Sargent, B.; Yet, L.; Kan, Y.; Palyha, O.; Kelly, T. M.; Guan, X.-M.; Rosko, K.; Gagen, K.; Metzger, J. M.; Dragovic, J.; Lyons, K.; Lin, L. S.; Nargund, R. P. Synthesis of 7-benzyl-5-(piperidin-1-yl)-6,7,8,9-tetrahydro-3H-pyrazolo[3,4-c]-[2,7]naphthyridin-1ylamine and its analogs as bombesin receptor subtype-3 agonists. *Bioorg. Med. Chem. Lett.* **2010,** *20*, 2785.
(10) He, S.; Dobbelaar, P. H.; Liu, J.; Jian, T.; Sebhat, I. K.; Lin, L. S.; Goodman, A.; Guo, C.; Guzzo, P. R.; Hadden, M.; Henderson, A. J.; Ruenz, M.; Sargent, B.; Yet, L.; Kelly, T. M.; Palyha, O.; Kan, Y.; Pan, J.; Chen, H.; Marsh, D.; Shearman, L. P.; Strack, A. M.; Metzger, J. M.; Feighner, S. D.; Tan, C.; Howard, A. D.; Tamvakopoulos, C.; Peng, Q.; Guan, X.-M.; Reitman, M. L.; Patchett, A. A.; Wyvratt, M. J.; Nargund, R. P. Discovery of substituted biphenyl imidazoles as potent bioavailable bombesin receptor subtype-3 agonists. *Bioorg. Med. Chem. Lett.* **2010,** *20*, 1913–1917.
(11) Liu, J.; He, S.; Jian, T.; Dobbelaar, P. H.; Sebhat, I. K.; Lin, L. S.; Goodman, A.; Guo, C.; Guzzo, P. R.; Hadden, M.; Henderson, A. J.; Pattamana, K.; Ruenz, M.; Sargent, B.; Swenson, B.; Yet, L.; Tamvakopoulos, C.; Peng, Q.; Pan, J.; Kan, Y.; Palyha, O.; Kelly, T. M.; Guan, X.-M.; Howard, A. D.; Marsh, D.; Metzger, J.; Reitman, M. L.; Wyvratt, M. J.; Nargund, R. P. Synthesis and SAR of derivatives based on 2-biarylethylimidazole as bombesin receptor subtype-3 (BRS-3) agonists for the treatment of obesity. *Bioorg. Med. Chem. Lett.* **2010,** *20*, 2074–2077.
(12) Hadden, M.; Goodman, A.; Guo, C.; Guzzo, P. R.; Henderson, A. J.; Pattamana, K.; Ruenz, M.; Sargent, B.; Swenson, B.; Yet, L.; Liu, J.; He, S.; Sebhat, I. K.; Lin, L. S.; Tamvakopoulos, C.; Peng, Q.; Kan, Y.; Palyha, O.; Kelly, T. M.; Guan, X.-M.; Metzger, J.; Reitman, M. L.; Nargund, R. P. Synthesis and SAR of heterocyclic carboxylic acid isosteres based on 2-biarylethylimidazole as bombesin receptor subtype-3 (BRS-3) agonists for the treatment of obesity. *Bioorg. Med. Chem. Lett.* **2010,** *20*, 2912–2915.
(13) Guan, X.-M.; Chen, H.; Dobbelaar, P. H.; Dong, Y.; Fong, T. M.; Gagen, K.; Gorski, J.; He, S.; Howard, A. D.; Jian, T.; Jiang, M.; Kan, Y.; Kelly, T. M.; Kosinski, J.; Lin, L. S.; Liu, J.; Marsh, D.; Metzger, J. M.; Miller, R.; Nargund, R. P.; Palyha, O.; Shearman, L.; Shen, Z.; Stearns, R.; Strack, A. M.; Stribling, S.; Tang, Y. S.; Wang, S.-P.; White, A.; Yu, H.; Reitman, M. L. Regulation of energy homeostasis by bombesin receptor subtype-3: Selective receptor agonists for the treatment of obesity. *Cell Metab.* **2010,** *11*, 101–112.
(14) Absolute stereochemistry was determined via X-ray crystallography of the hydrochloride salt of an iodinated analogue ((2*S*)-1,1,1-trifluoro-3-(5-iodo-4-{[1-(trifluoromethyl)cyclopropyl]-methyl}-1*H*-imidazol-2-yl)-2-[4-(1*H*-pyrazol-1-yl)phenyl]propan-2-ol). Crystals of this salt were grown by evaporation of an EtOAc/hexane solution over a period of approximately 1 week. Diffraction data were measured at room temperature. Examination of the intermolecular distances to the Cl ion as well as the electron density maps indicates the protonation by HCl to form the salt occurs at N23. With the presence of the two heavy atoms in the lattice, determination of the absolute configuration at the chiral C (C1, *S*) was unambiguous.
(15) Receptor binding was performed using membranes from CHO or HEK293 cells overexpressing the indicated receptor. A 30 pM concentration of [^{125}I]-[D-Tyr6,β-Ala^{11},Phe^{13},Nle^{14}]-bombesin(6−14) (human assay) and 660 pM [^{3}H]Bag-3 (rat and mouse assays) were used. For functional assays, agonist-induced mobilization of intracellular Ca^{2+} was measured in HEK293AEQ cells overexpressing BRS-3, using an aequorin bioluminescence assay.
(16) Guan, X.-M. Manuscript submitted.

DOI: 10.1021/ml100196d | *ACS Med. Chem. Lett.* **2011**, *2*, 43–47